Annales
Geophysicae

Seasonal dependence of the Earth's radiation belt – new insights

Rajkumar Hajra

Indian Institute of Technology Indore, Simrol, Indore 453552, India

Correspondence: Rajkumar Hajra (rajkumarhajra@yahoo.co.in)

Abstract. Long-term variations in the relativistic ($\sim$ MeV) electrons in the Earth's radiation belt are explored to study seasonal features of the electrons. An L-shell dependence of the seasonal variations in the electrons is reported for the first time. A clear $\sim$ 6 month periodicity, representing one/two peaks per year, is identified for 1.5–6.0 MeV electron fluxes in the L shells between $\sim$ 3.0 and $\sim$ 5.0. The relativistic electron flux variation is strongest during solar cycle descending to minimum phases, with weaker/no variations during solar maximum. If two peaks per year occur, they are largely asymmetric in amplitude. The peaks essentially do not have an equinoctial dependence. Sometimes the peaks are shifted to solstices, and sometimes only one annual peak is observed. No such seasonal features are prominent for $L < 3.0$ and $L > 5.0$. The results imply varying solar/interplanetary drivers of the radiation belt electrons at different L shells. This has a potential impact on the modeling of the space environment. Plausible solar drivers are discussed.

1 Introduction

Earth-orbiting satellites traversing through the radiation belts (Van Allen et al., 1958) are vulnerable to relativistic ($\sim$ MeV) electrons that can cause internal charging, leading to satellite component damage or even satellite loss in extreme cases (e.g., Wrenn, 1995; Iucci et al., 2005; Horne et al., 2013; Baker et al., 2018, and references therein). The MeV electrons in the outer radiation belt ($L > 2.5$) are known to be accelerated from the $\sim$ 10–100 keV (energetic) electrons which are injected into the nightside magnetosphere by substorms (e.g., DeForest and McIlwain, 1971; Horne and Thorne, 1998) and convection events in high-intensity, long-duration, continuous auroral electrojet (AE) activities (HILDCAAs; Tsurutani et al., 2004). The tem-

perature anisotropy of the electrons leads to plasma instability generating whistler-mode chorus waves (Kennel and Petschek, 1966; Tsurutani and Smith, 1974). Resonant interaction of the $\sim$ 100 keV electrons with chorus waves leads to MeV electron acceleration (Inan et al., 1978; Horne and Thorne, 2003; Summers et al., 2007; Tsurutani et al., 2013; Xiao et al., 2014; Foster et al., 2017; Matsui et al., 2017; Omura et al., 2019; Zhang et al., 2020).

From the above scenario, it is implied that the injections of seed ($\sim$ 10–100 keV) electrons through substorms/HILDCAAs, along with electron loss processes, control the variability in magnetospheric MeV electrons in the outer radiation belt. In other words, the solar wind–magnetosphere coupling processes that cause substorms and HILDCAAs, play an important role in MeV electron variability. The electrons are reported to vary in the timescales of a fraction of a second (e.g., microbursts; Tsurutani et al., 2013) to several years. While short-scale variations are attributed to wave–particle interactions and associated solar wind and interplanetary variations, long-term variations are associated with solar activity cycle (e.g., Baker et al., 1986; Tsurutani et al., 2006, 2016; Miyoshi and Kataoka, 2011; Hajra et al., 2013, 2014a, b, 2015a, b, 2020; Li et al., 2015; Hajra and Tsurutani, 2018). Several studies of MeV electrons (e.g., Baker et al., 1999; Li et al., 2001; Kanekal et al., 2010) reported strong semi-annual modulations of the electrons and discussed this in the context of the Earth's position in the heliosphere (Cortie, 1912), the relative angle of solar wind incidence with respect to Earth's rotation axis (Boller and Stolov, 1970), and the geometrical controls of interplanetary magnetic fields (Russell and McPherron, 1973). The aim of this present work is a critical exploration of the seasonal features of the MeV electrons and to identify their solar activity and L-shell dependencies, if any.

2   Data analysis and results

Figure 1a shows the variation in the monthly mean differential fluxes of the electrons in the energy range between 1.5 and 6.0 MeV in different L shells from 0.5 to 8.5 from July 1992 through June 2004. The L parameter is the radial distance in Earth radii at the magnetic equator for a dipole approximation of the Earth's magnetic field (McIlwain, 1961). An L^* parameter (Roederer, 1970) could have been used, but because most of the primary results pertain to $L < 5.0$, it is felt that the L parameter is reasonable to use for this effort. The electron observations are made by the Solar, Anomalous, and Magnetospheric Particle Explorer (SAMPEX; Baker et al., 1993) that monitored the radiation belts from a low-altitude (~ 520–670 km), highly (82°) inclined orbit. Figure 1a shows a classical picture of the Van Allen radiation belts – an inner belt with lower fluxes of 1.5–6.0 MeV electrons at $L < 2.0$, separated by a slot region devoid of any electrons up to $L \sim 2.5$, from an outer belt extending up to $L \sim 7.0$. Peak fluxes occur around $L \sim 3.0$–4.5, as shown by superposed black lines.

The MeV electron flux variations are compared with the monthly mean solar wind speed V_{sw} (Fig. 1b, red curve; see the legend on the right), the percentage occurrences of days with daily peak $V_{sw} \geq 500 \, \mathrm{km\,s^{-1}}$ (marked as D500; Fig. 1b, histograms; see the legend on the left), the monthly mean solar wind electric field VB_s (Fig. 1c), where V represents V_{sw}, and B_s is the southward component of the interplanetary magnetic field (IMF) or is zero in absence of the southward component. VB_s has been shown to be the main driver of geomagnetic activity (e.g., Burton et al., 1975; Tsurutani et al., 1992, 1995; Finch et al., 2008). Figure 1d shows the monthly mean F10.7 solar flux that depicts the ~ 11 year solar activity cycle. The period under study extends from the descending phase of solar cycle 22 to the descending phase of solar cycle 23. The solar wind and IMFs are obtained from the OMNI website (https://omniweb.gsfc.nasa.gov/, last access: 7 September 2020). The OMNI database is formed by time-shifting the observations made by the NASA's Advanced Composition Explorer (ACE), Wind, and Interplanetary Monitoring Platform 8 (IMP 8) spacecraft to the Earth's bow shock nose. The IMFs, in geocentric solar magnetospheric (GSM) coordinates, are used in this work.

An overall association of solar wind high-speed ($V_{sw} \geq 500 \, \mathrm{km\,s^{-1}}$) streams (HSSs) and MeV electron fluxes can be observed in the figure. Both V_{sw} and D500 exhibit two prominent peaks – one around 1994–1995 and another around 2003–2004 – which are in the descending phases of solar activity cycles 22 and 23, respectively. These intervals are characterized by flux enhancements and the broadening of the 1.5–6.0 MeV electron belt in L-shell space. On the other hand, a clear narrowing of the belt at lower L shells and flux decreases can be noted in the ascending and maximum phases of solar cycle 23. A close look in the fluxes reveals smaller-scale flux variations
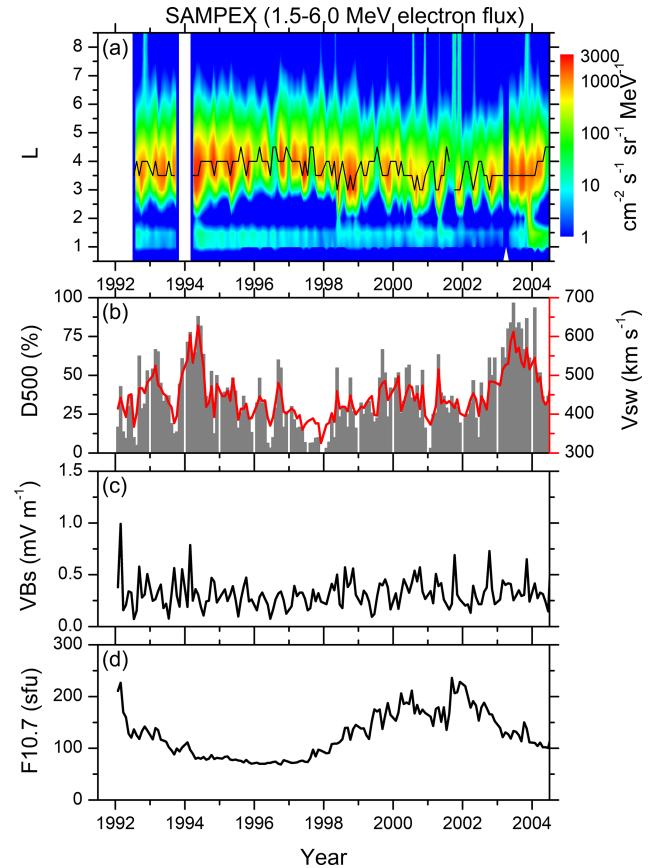

Figure 1. Panel **(a)** shows the L-shell variation of monthly mean differential 1.5–6.0 MeV electron fluxes (the legend on the right shows flux values corresponding to different colors) and L shells corresponding to peak fluxes (black curve), **(b)** the monthly percentage of days with peak solar wind speed $V_{sw} \geq 500 \, \mathrm{km\,s^{-1}}$ (the legend on the left) and monthly mean V_{sw} (red curve; see the legend on the right), **(c)** the monthly mean VB_s and **(d)** F10.7 solar flux for the years 1992 through 2004, respectively, and F10.7 is expressed in solar flux unit (sfu), where a sfu is $10^{-22} \, \mathrm{W\,m^{-2}\,Hz^{-1}}$.

in each year around the heart of the outer belt. A similar smaller-scale variation is recorded in VB_s.

Figure 2 shows Lomb–Scargle periodograms (Lomb, 1976; Scargle, 1982) of F10.7 solar flux, V_{sw}, D500, VB_s, and MeV electron fluxes at different L shells, as shown in Fig. 1. As expected, F10.7 exhibits a single periodicity of ~ 11 years depicting the solar activity cycle. Interestingly, V_{sw} has a broad peak around the 9.5 year period, with additional significant peaks at the ~ 4.6 and ~ 3.2 year periods. D500 exhibited a similar (to V_{sw}) periodogram. The coupling function VB_s is independent of solar activity and has a significant period of ~ 0.5 years or ~ 6 months only.
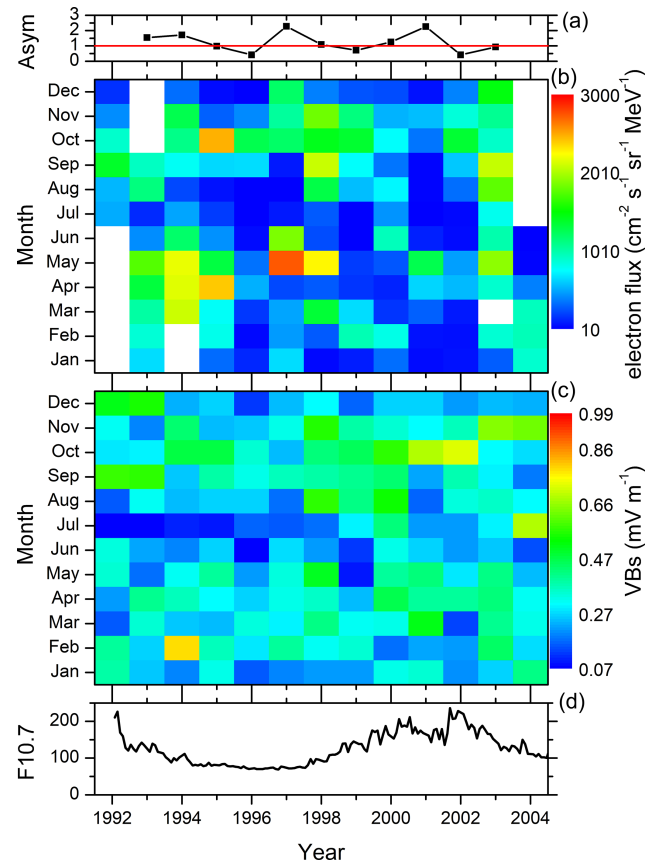
The electron fluxes at different L shells exhibit large variations in periodicity. At $L = 1.0$ (inner belt), electrons exhibit significant periods of ~ 8.9 and ~ 4.3 years. These seem to be associated with variations in V_{sw} (D500) with similar periods. However, it should be noted that electron measurement
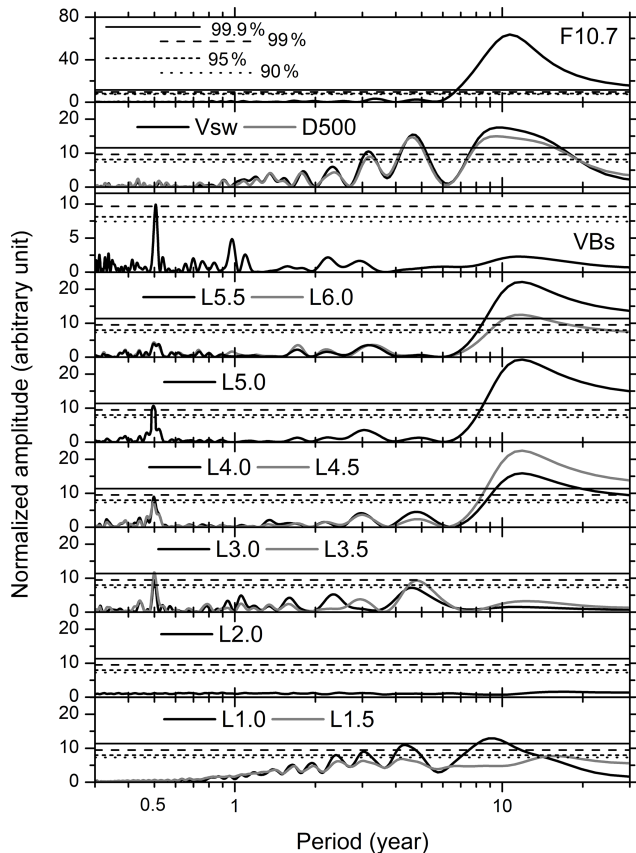
Figure 2. From top to bottom, the panels show Lomb–Scargle periodograms of F10.7, V_{sw} and D500, VB_s, and 1.5–6.0 MeV electron fluxes at different L shells. The x axis shows periods in year, and the y axis shows the normalized amplitudes in arbitrary unit. Confidence levels of the periodograms are shown in each panel by horizontal lines.

Figure 3. Contour plots in panels (**b**) and (**c**) show the monthly mean 1.5–6.0 MeV electron fluxes at $L = 3.5$ and monthly mean VB_s, respectively, during each month for the years 1992 through 2004. Panel (**a**) shows seasonal asymmetry (defined in the text), and panel (**d**) shows the F10.7 solar flux during the same interval.

in the inner belt are largely contaminated by very energetic (≥ 10–100 MeV) protons (see, e.g., Singer, 1958; Fennell et al., 2015; Selesnick et al., 2016, and references therein). For obvious reason, slot region ($L = 2.0$) electrons have no significant variation. At the inner edge of the outer belt ($L = 3.0$ and 3.5), electrons exhibit a significant periodicity of ~ 6 months but no periodicity related to the ~ 11 year solar activity cycle. In the shells between $L = 4.0$ and $L = 5.0$, an ~ 11 year periodicity is accompanied by a prominent periodicity of ~ 6 months. The ~ 6 month periodicity in the electrons (for $L = 3.0$ to 5.0) can be attributed to the variations in the coupling function VB_s. Electrons at $L = 5.5$ and 6.0 exhibit only a significant periodicity of ~ 11 years. At $L > 6.0$, there is no clear periodic variation in MeV electron fluxes.

Figure 2 clearly indicates varying solar activity and seasonal variations in the 1.5–6.0 MeV electrons at different L shells, which can be attributed to different solar and magnetospheric drivers. This will be discussed later in the paper.

Figure 3 shows the year–month contour plots of monthly mean MeV electron fluxes at $L = 3.5$ and monthly mean VB_s. The top panel shows the ratio of electron flux seasonal peaks in the two halves of each year. This may give an estimate of the seasonal asymmetry of the electron fluxes. It should be noted that the months of the peaks varied from year to year, which will be discussed below. The monthly mean F10.7 solar flux is repeated from Fig. 1 for a reference of solar activity cycle. Similar analysis is performed for electrons at other L shells; however, they are not shown here to avoid repetition and save space.

While Fig. 2 shows a ~ 6 month (semi-annual) component both in electron flux variation at $L = 3.5$ and in VB_s variation, a clear year-to-year variation can be observed in Fig. 3. In the year 1993, electron fluxes peak around May and August, while two peaks are observed during the months of May and November in 1994. In both cases, the first peaks are ~ 1.5–1.7 times higher than the second peaks. In April and October 1995, the two electron flux peaks are much more distinct and comparable in amplitude. The semi-annual varia-

tion is much weaker in 1996, with a peak in April ~ 0.5 times of that in October. In 1997, a large peak in fluxes can be noted in May with no prominent equinoctial peaks. In 1998, which is in the ascending phase of solar cycle 23, two distinct and comparable peaks are recorded during May and September. In 1999, while electron fluxes are much lower, two peaks can be noted in February and October. No clear seasonal feature can be inferred from 2000, while a solstice peak (May) is observed in 2001 and an October peak in 2002. A two-peak seasonal feature, with two distinct and comparable peaks in May and September, is again observed in 2003 in the descending phase of solar cycle 23. A consistent variation is observed in VB_s with respect to month and year.

It can be concluded from the above analysis that, while the 1.5–6.0 MeV electron fluxes at $L = 3.5$ exhibit mostly two peaks in a year, they are largely asymmetric in amplitude, and they are not essentially equinoctial. The same conclusions were drawn for electrons at other L shells.

3   Discussion and conclusions

The results of this paper reveal that the MeV electrons in the Earth's outer zone radiation belt exhibit varying solar and seasonal features, depending on the L shells. No ~ 11 year solar cycle trend was observed in the inner edge ($L = 3.0$–3.5) of the outer belt, where a dominating ~ 6 month period was prominent. From $L = 4.0$ to 5.0, the ~ 11 year solar cycle variation is accompanied by a secondary ~ 6 month period. Electrons at $L = 5.5$ and 6.0 exhibit only a significant periodicity of ~ 11 years, above which there are no clear periodic variations in MeV electron fluxes. These L-shell-dependent seasonal and solar cycle features are reported for the first time. These are in contrast to previous studies (e.g., Baker et al., 1999; Li et al., 2001; Kanekal et al., 2010) that reported strong and coherent seasonal modulations of MeV electrons throughout the entire outer zone radiation belt.

Interestingly, no ~ 6 month component was observed in solar wind speed V_{sw}, while it was most prominent in the solar wind–magnetospheric coupling function VB_s which represents the interplanetary electric field under the condition of southward IMFs. This implies that the seasonal feature is due to magnetic configuration (B_s). In addition, the absence of a periodic component in V_{sw} below a period of a few years is of interest, and it shows that the solar wind activity is intrinsically aperiodic on these timescales so that the observed seasonal dependency can only be proper to the geospheric system (which is compatible with the usual explanation of the seasonal effect). The above result is consistent with previous results (e.g., Li et al., 2011), suggesting that HSSs alone cannot predict relativistic electron flux enhancements, but that fast solar wind and southward IMFs are the main requirements for electron enhancements. This makes VB_s, involving both solar wind speed and southward IMF, an important factor controlling MeV electron variation.

However, the present study involving multi-year analysis of seasonal features in MeV electrons and solar/magnetospheric drivers reveals that care should be taken in interpreting the ~ 6 month periodicity obtained through periodogram analysis (present work) or superposed analysis of electrons in the radiation belt (previous reports). The two yearly peaks in the electron fluxes (between $L = 3.0$ and 5.0) are only sometimes observed around descending phase of the solar cycle. The peaks are largely asymmetric in nature. In addition, the peaks are essentially not equinoctial; sometimes the peaks are shifted to solstices, and sometimes only one annual peak is observed. Clearly the ~ 6 month periodicity in the periodogram (and semi-annual variation) of the magnetospheric MeV electrons is an artifact arising from long-term data superposition in years. That the seasonal effects are statistical in nature, and that they apply to the geoeffectiveness of the solar/interplanetary drivers, is now well understood (see, Cliver et al., 2000, 2004; Nowada et al., 2009; Mursula et al., 2011; Cnossen and Richmond, 2012; Lockwood et al., 2020; Tsurutani et al., 2020, and references therein). However, when applying axial, equinoctial, or geometrical hypotheses to discuss the Earth's radiation belt, the importance of the solar cycle period component and the impact of V_{sw} should be considered. In addition, radiation belt dynamics are strongly dependent on the energy of the electrons. Thus, the energy dependence on the seasonal variations should also be investigated for a more complete understanding.

In summary, the L-shell-dependent solar and seasonal features and so-called semi-annual variations in magnetospheric relativistic electrons require further attention. Dual satellite Van Allen Probes (Mauk et al., 2013) involving multi-energy observations of the radiation belts can be useful for further confirmation of the results obtained in the present work.

References

Baker, D. N., Blake, J. B., Klebesadel, R. W., and Higbie, P. R.: Highly relativistic electrons in the Earth's outer magnetosphere: 1. Lifetimes and temporal history 1979–1984, J. Geophys. Res.-Space, 91, 4265–4276, https://doi.org/10.1029/JA091iA04p04265, 1986.

Baker, D. N., Mason, G. M., Figueroa, O., Colon, G., Watzin, J. G., and Aleman, R. M.: An overview of the Solar Anomalous, and Magnetospheric Particle Explorer (SAMPEX) mission, IEEE T. Geosci Remote, 31, 531–541, 1993.

Baker, D. N., Kanekal, S. G., Pulkkinen, T. I., and Blake, J. B.: Equinoctial and solstitial averages of magnetospheric relativistic electrons: A strong semiannual modulation, Geophys. Res. Lett., 26, 3193–3196, https://doi.org/10.1029/1999GL003638, 1999.

Baker, D. N., Erickson, P. J., Fennell, J. F., Foster, J. C., Jaynes, A. N., and Verronen, P. T.: Space Weather Effects in the Earth's Radiation Belts, Space Sci. Rev., 214, https://doi.org/10.1007/s11214-017-0452-7, 2018.

Boller, B. R. and Stolov, H. L.: Kelvin–Helmholtz instability and the semiannual variation of geomagnetic activity, J. Geophys. Res.-Space, 75, 6073–6084, https://doi.org/10.1029/JA075i031p06073, 1970.

Burton, R. K., McPherron, R. L., and Russell, C. T.: An empirical relationship between interplanetary conditions and Dst, J. Geophys. Res.-Space, 80, 4204–4214, https://doi.org/10.1029/JA080i031p04204, 1975.

Cliver, E. W., Kamide, Y., and Ling, A. G.: Mountains versus valleys: Semiannual variation of geomagnetic activity, J. Geophys. Res.-Space, 105, 2413–2424, https://doi.org/10.1029/1999JA900439, 2000.

Cliver, E. W., Svalgaard, L., and Ling, A. G.: Origins of the semiannual variation of geomagnetic activity in 1954 and 1996, Ann. Geophys., 22, 93–100, https://doi.org/10.5194/angeo-22-93-2004, 2004.

Cnossen, I. and Richmond, A. D.: How changes in the tilt angle of the geomagnetic dipole affect the coupled magnetosphere-ionosphere-thermosphere system, J. Geophys. Res.-Space, 117, A10317, https://doi.org/10.1029/2012JA018056, 2012.

Cortie, A. L.: Sun-spots and Terrestrial Magnetic Phenomena, 1898–1911: the Cause of the Annual Variation in Magnetic Disturbances, Mon. Not. R. Astron. Soc., 73, 52–60, https://doi.org/10.1093/mnras/73.1.52, 1912.

DeForest, S. E. and McIlwain, C. E.: Plasma clouds in the magnetosphere, J. Geophys. Res.-Space, 76, 3587–3611, https://doi.org/10.1029/JA076i016p03587, 1971.

Fennell, J. F., Claudepierre, S. G., Blake, J. B., O'Brien, T. P., Clemmons, J. H., Baker, D. N., Spence, H. E., and Reeves, G. D.: Van Allen Probes show that the inner radiation zone contains no MeV electrons: ECT/MagEIS data, Geophys. Res. Lett., 42, 1283–1289, https://doi.org/10.1002/2014GL062874, 2015.

Finch, I. D., Lockwood, M. L., and Rouillard, A. P.: Effects of solar wind magnetosphere coupling recorded at different geomagnetic latitudes: Separation of directly-driven and storage/release systems, Geophys. Res. Lett., 35, L21105, https://doi.org/10.1029/2008GL035399, 2008.

Foster, J. C., Erickson, P. J., Omura, Y., Baker, D. N., Kletzing, C. A., and Claudepierre, S. G.: Van Allen Probes observations of prompt MeV radiation belt electron acceleration in nonlinear interactions with VLF chorus, J. Geophys. Res.-Space, 122, 324–339, https://doi.org/10.1002/2016JA023429, 2017.

Hajra, R. and Tsurutani, B. T.: Chapter 14 – Magnetospheric "Killer" Relativistic Electron Dropouts (REDs) and Repopulation: A Cyclical Process, in: Extreme Events in Geospace: Origins, Predictability, and Consequences, edited by: Buzulukova, N., Elsevier, the Netherlands, 373–400, https://doi.org/10.1016/B978-0-12-812700-1.00014-5, 2018.

Hajra, R., Echer, E., Tsurutani, B. T., and Gonzalez, W. D.: Solar cycle dependence of High-Intensity Long-Duration Continuous AE Activity (HILDCAA) events, relativistic electron predictors?, J. Geophys. Res.-Space, 118, 5626–5638, https://doi.org/10.1002/jgra.50530, 2013.

Hajra, R., Echer, E., Tsurutani, B. T., and Gonzalez, W. D.: Superposed epoch analyses of HILDCAAs and their interplanetary drivers: Solar cycle and seasonal dependences, J. Atmos. Sol.-Terr. Phy., 121, 24–31, https://doi.org/10.1016/j.jastp.2014.09.012, 2014a.

Hajra, R., Tsurutani, B. T., Echer, E., and Gonzalez, W. D.: Relativistic electron acceleration during high-intensity, long-duration, continuous AE activity (HILDCAA) events: Solar cycle phase dependences, Geophys. Res. Lett., 41, 1876–1881, https://doi.org/10.1002/2014GL059383, 2014b.

Hajra, R., Tsurutani, B. T., Echer, E., Gonzalez, W. D., Brum, C. G. M., Vieira, L. E. A., and Santolik, O.: Relativistic electron acceleration during HILDCAA events: are precursor CIR magnetic storms important?, Earth Planets Space, 67, 109, https://doi.org/10.1186/s40623-015-0280-5, 2015a.

Hajra, R., Tsurutani, B. T., Echer, E., Gonzalez, W. D., and Santolik, O.: Relativistic (E > 0.6, > 2.0, and > 4.0 MeV) electron acceleration at geosynchronous orbit during high-intensity, long-duration, continuous AE activity (HILDCAA) events, Astrophys. J., 799, 39, https://doi.org/10.1088/0004-637x/799/1/39, 2015b.

Hajra, R., Tsurutani, B. T., and Lakhina, G. S.: The Complex Space Weather Events of 2017 September, Astrophys. J., 899, 3, https://doi.org/10.3847/1538-4357/aba2c5, 2020.

Horne, R. B. and Thorne, R. M.: Potential waves for relativistic electron scattering and stochastic acceleration during magnetic storms, Geophys. Res. Lett., 25, 3011–3014, https://doi.org/10.1029/98GL01002, 1998.

Horne, R. B. and Thorne, R. M.: Relativistic electron acceleration and precipitation during resonant interactions with whistler-mode chorus, Geophys. Res. Lett., 30, https://doi.org/10.1029/2003GL016973, 2003.

Horne, R. B., Glauert, S. A., Meredith, N. P., Boscher, D., Maget, V., Heynderickx, D., and Pitchford, D.: Space weather impacts on satellites and forecasting the Earth's electron radiation belts with SPACECAST, Space Weather, 11, 169–186, https://doi.org/10.1002/swe.20023, 2013.

Inan, U. S., Bell, T. F., and Helliwell, R. A.: Nonlinear pitch angle scattering of energetic electrons by coherent VLF waves in the magnetosphere, J. Geophys. Res.-Space, 83, 3235–3253, https://doi.org/10.1029/JA083iA07p03235, 1978.

Iucci, N., Levitin, A. E., Belov, A. V., Eroshenko, E. A., Ptitsyna, N. G., Villoresi, G., Chizhenkov, G. V., Dorman, L. I., Gromova, L. I., Parisi, M., Tyasto, M. I., and Yanke, V. G.: Space weather conditions and spacecraft anomalies in different orbits, Space Weather, 3, S01001, https://doi.org/10.1029/2003SW000056, 2005.

Kanekal, S. G., Baker, D. N., and McPherron, R. L.: On the seasonal dependence of relativistic electron fluxes, Ann. Geophys., 28, 1101–1106, https://doi.org/10.5194/angeo-28-1101-2010, 2010.

Kennel, C. F. and Petschek, H. E.: Limit on stably trapped particle fluxes, J. Geophys. Res.-Space, 71, 1–28, https://doi.org/10.1029/JZ071i001p00001, 1966.

Li, W., Thorne, R. M., Bortnik, J., Baker, D. N., Reeves, G. D., Kanekal, S. G., Spence, H. E., and Green, J. C.: Solar wind conditions leading to efficient radiation belt electron acceleration: A superposed epoch analysis, Geophys. Res. Lett., 42, 6906–6915, https://doi.org/10.1002/2015GL065342, 2015.

Li, X., Baker, D. N., Kanekal, S. G., Looper, M., and Temerin, M.: Long term measurements of radiation belts by SAMPEX and their variations, Geophys. Res. Lett., 28, 3827–3830, https://doi.org/10.1029/2001GL013586, 2001.

Li, X., Temerin, M., Baker, D. N., and Reeves, G. D.: Behavior of MeV electrons at geosynchronous orbit during last two solar cycles, J. Geophys. Res.-Space, 116, A11207, https://doi.org/10.1029/2011JA016934, 2011.

Lockwood, M., Owens, M. J., Barnard, L. A., Haines, C., Scott, C. J., McWilliams, K. A., and Coxon, J. C.: Semi-annual, annual and Universal Time variations in the magnetosphere and in geomagnetic activity: 1. Geomagnetic data, J. Space Weather Spac., 10, 23, https://doi.org/10.1051/swsc/2020023, 2020.

Lomb, N. R.: Least-squares frequency analysis of unequally spaced data, Astrophys. Space Sci., 39, 447–462, https://doi.org/10.1007/BF00648343, 1976.

Matsui, H., Torbert, R. B., Spence, H. E., Argall, M. R., Alm, L., Farrugia, C. J., Kurth, W. S., Baker, D. N., Blake, J. B., Funsten, H. O., Reeves, G. D., Ergun, R. E., Khotyaintsev, Y. V., and Lindqvist, P.-A.: Relativistic Electron Increase During Chorus Wave Activities on the 6–8 March 2016 Geomagnetic Storm, J. Geophys. Res.-Space, 122, 11302–11319, https://doi.org/10.1002/2017JA024540, 2017.

Mauk, B. H., Fox, N. J., Kanekal, S. G., Kessel, R. L., Sibeck, D. G., and Ukhorskiy, A.: Science Objectives and Rationale for the Radiation Belt Storm Probes Mission, Space Sci. Rev., 179, 3–27, https://doi.org/10.1007/s11214-012-9908-y, 2013.

McIlwain, C. E.: Coordinates for mapping the distribution of magnetically trapped particles, J. Geophys. Res.-Space, 66, 3681–3691, https://doi.org/10.1029/JZ066i011p03681, 1961.

Miyoshi, Y. and Kataoka, R.: Solar cycle variations of outer radiation belt and its relationship to solar wind structure dependences, J. Atmos. Sol.-Terr. Phy., 73, 77–87, https://doi.org/10.1016/j.jastp.2010.09.031, 2011.

Mursula, K., Tanskanen, E., and Love, J. J.: Spring-fall asymmetry of substorm strength, geomagnetic activity and solar wind: Implications for semiannual variation and solar hemispheric asymmetry, Geophys. Res. Lett., 38, L06104, https://doi.org/10.1029/2011GL046751, 2011.

NASA: CDAWeb Selector Error, CDAWeb, available at: https://cdaweb.gsfc.nasa.gov/cgi-bin/eval1.cgi (last access: 7 September 2020), 2020a.

NASA: Paths to Magnetic field, Plasma, Energetic particle data relevant to heliospheric studies and resident at Goddard's Space Physics Data Facility, available at: https://omniweb.gsfc.nasa.gov/ (last access: 7 September 2020), 2020b.

Nowada, M., Shue, J. H., and Russell, C. T.: Effects of dipole tilt angle on geomagnetic activity, Planet. Space Sci., 57, 1254–1259, https://doi.org/10.1016/j.pss.2009.04.007, 2009.

Omura, Y., Hsieh, Y.-K., Foster, J. C., Erickson, P. J., Kletzing, C. A., and Baker, D. N.: Cyclotron Acceleration of Relativistic Electrons Through Landau Resonance With Obliquely Propagating Whistler-Mode Chorus Emissions, J. Geophys. Res.-Space, 124, 2795–2810, https://doi.org/10.1029/2018JA026374, 2019.

Roederer, J. G.: Dynamics of Geomagnetically Trapped Radiation, Vol. 2, Springer, Berlin, Heidelberg, https://doi.org/10.1007/978-3-642-49300-3, 1970.

Russell, C. T. and McPherron, R. L.: Semiannual variation of geomagnetic activity, J. Geophys. Res.-Space, 78, 92–108, https://doi.org/10.1029/JA078i001p00092, 1973.

Scargle, J. D.: Studies in astronomical time series analysis. II. Statistical aspects of spectral analysis of unevenly spaced data, Astrophys. J., 263, 835–853, 1982.

Selesnick, R. S., Su, Y.-J., and Blake, J. B.: Control of the innermost electron radiation belt by large-scale electric fields, J. Geophys. Res.-Space, 121, 8417–8427, https://doi.org/10.1002/2016JA022973, 2016.

Singer, S. F.: Trapped Albedo Theory of the Radiation Belt, Phys. Rev. Lett., 1, 181–183, https://doi.org/10.1103/PhysRevLett.1.181, 1958.

Summers, D., Ni, B., and Meredith, N. P.: Timescales for radiation belt electron acceleration and loss due to resonant wave-particle interactions: 2. Evaluation for VLF chorus, ELF hiss, and electromagnetic ion cyclotron waves, J. Geophys. Res.-Space, 112, A04207, https://doi.org/10.1029/2006JA011993, 2007.

Tsurutani, B. T. and Smith, E. J.: Postmidnight chorus: A substorm phenomenon, J. Geophys. Res.-Space, 79, 118–127, https://doi.org/10.1029/JA079i001p00118, 1974.

Tsurutani, B. T., Gonzalez, W. D., Tang, F., and Lee, Y. T.: Great magnetic storms, Geophys. Res. Lett., 19, 73–76, https://doi.org/10.1029/91GL02783, 1992.

Tsurutani, B. T., Gonzalez, W. D., Gonzalez, A. L. C., Tang, F., Arballo, J. K., and Okada, M.: Interplanetary origin of geomagnetic activity in the declining phase of the solar cycle, J. Geophys. Res.-Space, 100, 21717–21733, https://doi.org/10.1029/95JA01476, 1995.

Tsurutani, B. T., Gonzalez, W. D., Guarnieri, F., Kamide, Y., Zhou, X., and Arballo, J. K.: Are high-intensity long-duration continuous AE activity (HILDCAA) events substorm expansion events?, J. Atmos. Sol.-Terr. Phy., 66, 167–176, https://doi.org/10.1016/j.jastp.2003.08.015, 2004.

Tsurutani, B. T., Gonzalez, W. D., Gonzalez, A. L. C., Guarnieri, F. L., Gopalswamy, N., Grande, M., Kamide, Y., Kasahara, Y., Lu, G., Mann, I., McPherron, R., Soraas, F., and Vasyliunas, V.: Corotating solar wind streams and recurrent geomagnetic activity: A review, J. Geophys. Res.-Space, 111, A07S01, https://doi.org/10.1029/2005JA011273, 2006.

Tsurutani, B. T., Lakhina, G. S., and Verkhoglyadova, O. P.: Energetic electron (> 10 keV) microburst precipitation, $\sim$ 5–15 s X-ray pulsations, chorus, and wave-particle interac-

tions: A review, J. Geophys. Res.-Space, 118, 2296–2312, https://doi.org/10.1002/jgra.50264, 2013.

Tsurutani, B. T., Hajra, R., Tanimori, T., Takada, A., Remya, B., Mannucci, A. J., Lakhina, G. S., Kozyra, J. U., Shiokawa, K., Lee, L. C., Echer, E., Reddy, R. V., and Gonzalez, W. D.: Heliospheric plasma sheet (HPS) impingement onto the magnetosphere as a cause of relativistic electron dropouts (REDs) via coherent EMIC wave scattering with possible consequences for climate change mechanisms, J. Geophys. Res.-Space, 121, 10130–10156, https://doi.org/10.1002/2016JA022499, 2016.

Tsurutani, B. T., Lakhina, G. S., and Hajra, R.: The physics of space weather/solar-terrestrial physics (STP): what we know now and what the current and future challenges are, Nonlin. Processes Geophys., 27, 75–119, https://doi.org/10.5194/npg-27-75-2020, 2020.

Van Allen, J. A., Ludwig, G. H., Ray, E. C., and McIlwain, C. E.: Observation of High Intensity Radiation by Satellites 1958 Alpha and Gamma, Jet Propulsion, 28, 588–592, https://doi.org/10.2514/8.7396, 1958.

Wrenn, G. L.: Conclusive evidence for internal dielectric charging anomalies on geosynchronous communications spacecraft, J. Spacecraft Rockets, 32, 514–520, https://doi.org/10.2514/3.26645, 1995.

Xiao, F., Yang, C., He, Z., Su, Z., Zhou, Q., He, Y., Kletzing, C. A., Kurth, W. S., Hospodarsky, G. B., Spence, H. E., Reeves, G. D., Funsten, H. O., Blake, J. B., Baker, D. N., and Wygant, J. R.: Chorus acceleration of radiation belt relativistic electrons during March 2013 geomagnetic storm, J. Geophys. Res.-Space, 119, 3325–3332, https://doi.org/10.1002/2014JA019822, 2014.

Zhang, Z., Chen, L., Liu, S., Xiong, Y., Li, X., Wang, Y., Chu, W., Zeren, Z., and Shen, X.: Chorus Acceleration of Relativistic Electrons in Extremely Low L-Shell During Geomagnetic Storm of August 2018, Geophys. Res. Lett., 47, e2019GL086226, https://doi.org/10.1029/2019GL086226, 2020.